Finite Difference Analysis and Experimental Validation of 3D Photonic Crystals for Structural Health Monitoring

Valentina PICCOLO [1,2], Andrea CHIAPPINI [3], Alessandro VACCARI [4], Antonino CALA' LESINA[5], Maurizio FERRARI [3], Luca DESERI [1,2,7,8,9], Marcus PERRY[6], Daniele ZONTA [1,3,6]

[1] DICAM – Department of Civil, Environmental and Mechanical Engineering, University of Trento, Via Mesiano 77, 38123, Trento, Italy
[2] MEMS-Swanson School of Engineering, University of Pittsburgh Benedum Hall, 3700 O'Hara Street, Pittsburgh, PA 15261 USA
[3] Institute for Photonics and Nanotechnologies, National Research Council, Via alla Cascata 56/C, 38123 Trento, Italy
[4] Fondazione Bruno Kessler, Via Sommarive, 18, 38123, Trento, Italy
[5]Department of Physics, University of Ottawa, Ottawa, Ontario K1N 6N5, Canada
[6] University of Strathclyde Glasgow, 16 Richmond St, Glasgow G1 1XQ, United Kingdom
[7] MACE-Div. Aerospace Engineering, College of Engineering, Design and Physical Sciences, Brunel University London, Uxbridge, UB8 3PH, United Kingdom
[8] Dept. of Mech.Eng. Carnegie Mellon University, Pittsburgh PA 15213-3890 USA
[9] Department of Nanomedicine, The Methodist Hospital Research Institute, 6565 Fannin St., MS B-490 Houston, TX 77030 USA

Keywords: Smart Structure, 3D Colloidal Photonic Crystals, FDTD Simulations, Experimental Validation

ABSTRACT

In this work, we validate the behavior of 3D Photonic Crystals for Structural Health Monitoring applications. A Finite Difference Time Domain (FDTD) analysis has been performed and compared to experimental data. We demonstrate that the photonic properties of a crystal (comprised of sub-micrometric polystyrene colloidal spheres embedded in a PDMS matrix) change as a function of the axial strain applied to a rubber substrate. The change in the reflected wavelength, detected through our laboratory experiments and equivalent to a visible change in crystal color, is assumed to be caused by changes in the interplanar spacing of the polystyrene beads. This behavior is captured by our full wave 3D FDTD model. This contains different wavelengths in the visible spectrum and the wave amplitudes of the reflected and transmitted secondary beams are then computed. A change in the reflectance or transmittance is observed at every programmed step in which we vary the distance between the spheres. These investigations are an important tool to predict, study and validate our understanding of the behavior of this highly complex physical system. In this context, we have developed a versatile and robust parallelized code, able to numerically model the interaction of light with matter, by directly solving Maxwell's equations in their strong form. The ability to describe the physical behavior of such systems is an important and fundamental capability which will aid the design and validation of innovative photonic sensors.

Sensors and Smart Structures Technologies for Civil, Mechanical, and Aerospace Systems 2017, edited by Jerome P. Lynch, Proc. of SPIE Vol. 10168, 101681E · © 2017 SPIE
CCC code: 0277-786X/17/$18 · doi: 10.1117/12.2263975

1. INTRODUCTION

Structural Health Monitoring (SHM) is an important maintenance technology for civil infrastructures, such as bridges, towers, buildings, tunnels, dams and highway roads, as well as for mechanical and aerospace devices. This discipline is widespread in developed countries, like the USA and Europe, and it is used not only for newly built structures but also for historical heritage. Nowadays, the most commonly used techniques for obtaining SHM data are optical fiber Bragg grating and electronic strain gauges [1-6], but a major limitation to the widespread application of SHM are additional costs of the sensor network. In order to monitoring a large number of buildings an innovative a low cost technology is required. Strain imaging by visible light could be one of the possible answers, in fact is well known in the field of the photo-mechanics. In this research field, there are many techniques to visualize strain distribution of deforming structure, i.e. moiré interferometry, holography, image analysis, speckles and etc. [7].
Recently, the study of nano-structured materials paved the way for new device for strain or stress sensing. Between these new mechano-chromatic materials, in this work we will present the possible use of colloidal photonic crystal as strain sensors, due to the fact that they change color when subjected to strain [8-12]. We will also try to give a possible explanation of their behavior in terms of their reflected spectra, whenever such devices undergo imposed deformations. To this end, we perform numerical simulations that will not only help us to understand the possible configuration of the deformed nanostructure, but will also eventually allow us to design new strain sensors.

2. APPROXIMATE ANALYTICAL OPTOMECHANICAL SOLUTION

Consider the 3D photonic crystal schematically depicted in Fig.1b, made of colloidal spheres in an elastomeric matrix of refractive indices n_1 and n_2, respectively, and filling factor f. Illuminated by white light with zero incidence angle, the crystal reflects light around a specific band-gap wavelength λ. As a first approximation this is expressed by Bragg's law [13]:

$$\lambda = 2 \cdot n_{eff} \cdot d \tag{1}$$

where d is interplanar distance and n_{eff} is the effective refractive index of the crystal, for which a mixture theory-like approximation is adopted, namely:

$$n_{eff}^2 = f \cdot n_1^2 + (1-f) n_2^2 \tag{2}$$

Thus, a "small" change in the interplanar spacing d will result in a change in reflected wavelength according to:

$$\Delta\lambda = 2 \cdot n_{eff} \cdot \Delta d = 2 \cdot n_{eff} \cdot d_0 \cdot \varepsilon_3 \tag{3}$$

where ε_3 is the crystal (small) strain in the direction orthogonal to its plane and d_0 is the interplanar spacing in unstrained condition. This method applies in the context of infinitesimal strain. The crystal is adherent to a substrate and it is subject to a plain stress condition. Obviously the vertical contraction is related to the two in-plane strain components of the substrate through the following relationship:

$$\varepsilon_3 = -\frac{\nu}{1-\nu}\{\varepsilon_1 + \varepsilon_2\} \tag{4}$$

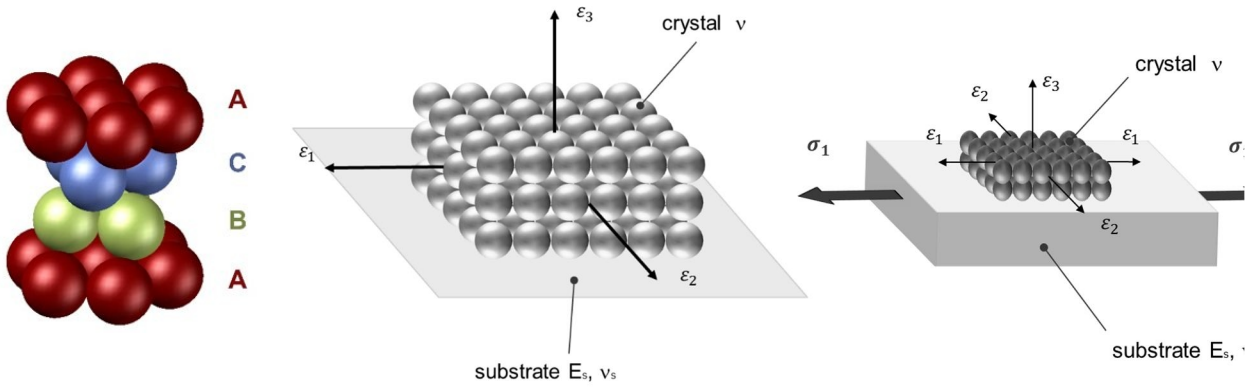

Figure 1. (a) 3D representation of the FCC structure of the opal photonic crystal; b) three dimensional photonic crystal on the substrate without stress application; c) the same configuration with stress applied (σ_1) and related to them strain distribution (ε_1, ε_2, ε_3); E_s, ν_s are Young modulus and Poisson's ratio for substrate, ν Poisson's ratio for photonic crystal.

If we apply a stress σ_1 to the substrate in direction 1, this will result in an elongation ε_1 in the same direction and in two contractions in the two orthogonal directions. With the assumption of effective isotropy of the composite matrix-spheres, the strain in the same plane of the substrate, ε_2, can be evaluated with the following formula:

$$\varepsilon_2 = -\nu_s \varepsilon_1, \tag{5}$$

where ν_s is and Poisson's coefficient of the substrate. Replacing (5) in (4), we obtain:

$$\varepsilon_3 = -\nu \frac{1-\nu_s}{1-\nu} \varepsilon_1 \approx -\nu \varepsilon_1 \tag{6}$$

where the approximation is valid as long as the two Poisson's ratios are close enough. Equation 6 basically states that when the substrate is stretched under a uniaxial stress in one in-plane direction, the crystal contracts approximately ν times the elongation along the stress direction. Combining (6) with (3) we finally determine the following expression for change in reflected wavelength $\Delta\lambda$:

$$\Delta\lambda \approx -2 \cdot n_{eff} \cdot \nu \cdot d_0 \cdot \varepsilon_1 \tag{7}$$

It is not clear whether or not the approximation of having an isotropic response is a too crude approximation, but this point will be discussed in section 4. In the most general case both the refractive index n_{eff} and Poisson's ratio ν could change with strain. Henceforth, the relationship between the bandgap wavelength and the transverse strain becomes nonlinear. In this case the sensitivity of $\Delta\lambda$ with the change in longitudinal strain takes approximately the following form:

$$\frac{\mathrm{d}\lambda}{\mathrm{d}\varepsilon_1} \approx -2 \cdot d_0 \cdot \left\{ \frac{\mathrm{d}n_{eff}}{\mathrm{d}\varepsilon_1} \cdot \nu \cdot \varepsilon_1 + n_{eff} \cdot \frac{\mathrm{d}\varepsilon_3}{\mathrm{d}\varepsilon_1} \right\}. \tag{8}$$

By assuming a linearly elastic behavior of the material and the effective refraction index n_{eff} constant with strain, equation (8) reduces to the following expression:

$$\frac{d\lambda}{d\varepsilon_1} \approx -2 \cdot n_{eff} \cdot \nu \cdot d_0 \quad , \tag{9}$$

which basically shows that the crystal sensitivity to strain is proportional to its refractive index, lattice spacing and Poisson's ratio.

3. MATERIALS AND METHODS

A prototype of colloidal Photonic Crystal (PhC) was fabricated and tested in the laboratory. The crystal, of dimensions 10×10 mm, was manufactured through deposition over a 50×15×1 mm rubber substrate of 230 nm polystyrene spheres, infiltrated with poly-dimethylsiloxane (PDMS). Details of the fabrication process are reported in [14]. Figure 2a shows a Scanning Electron Microscopy (SEM) image of the PhC: the interplanar spacing is 280 nm, resulting in a bandgap wavelength of 582 nm.

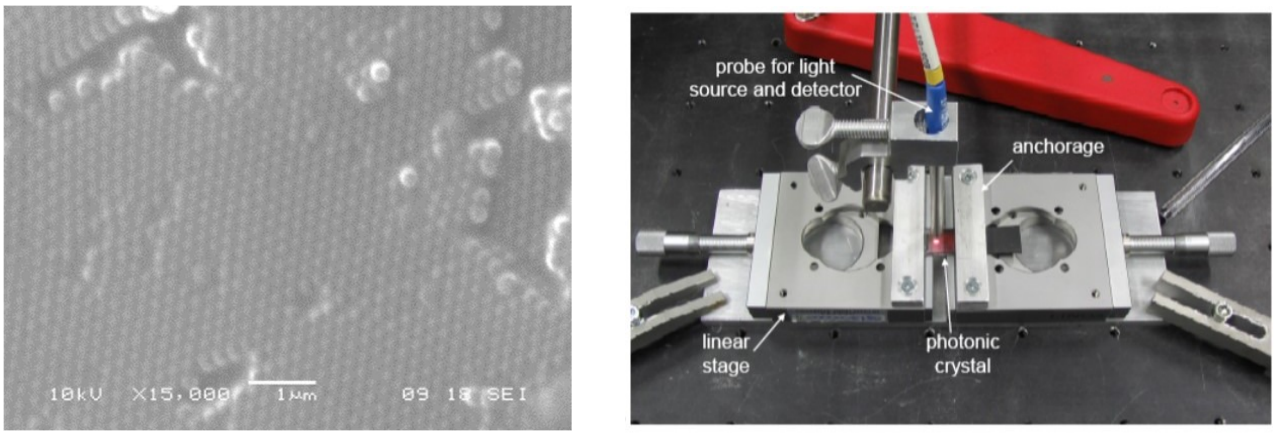

a) b)

Figure 2. (a) Scanning Electron Microscopy (SEM) picture of the crystal and (b) test setup [10].

During the test, the substrate strip was fastened to two micrometric linear stages, as shown in Figure 2b, and stretched in uniaxial condition to different strain levels. At each step, the reflectance of the PhC in the visible range using a spectrometer was recorded with a wavelength resolution of 0.1nm. Figure 3 a) shows the reflectance obtained for different values of the longitudinal strain, while Fig.3b plots the experimental relationship between reflectance peak wavelength and strain, as recorded during the test. As predicted by Equation (9), the wavelength decreases with strain and, below 120 mε, the relationship is approximately linear. In particular, the experimental sensitivity to strain and its inverse are:

$$\frac{d\lambda}{d\varepsilon} = \text{-0.288 pm/με} \; ; \quad \frac{d\varepsilon}{d\lambda} = \text{-3.47 με /pm} \tag{10}$$

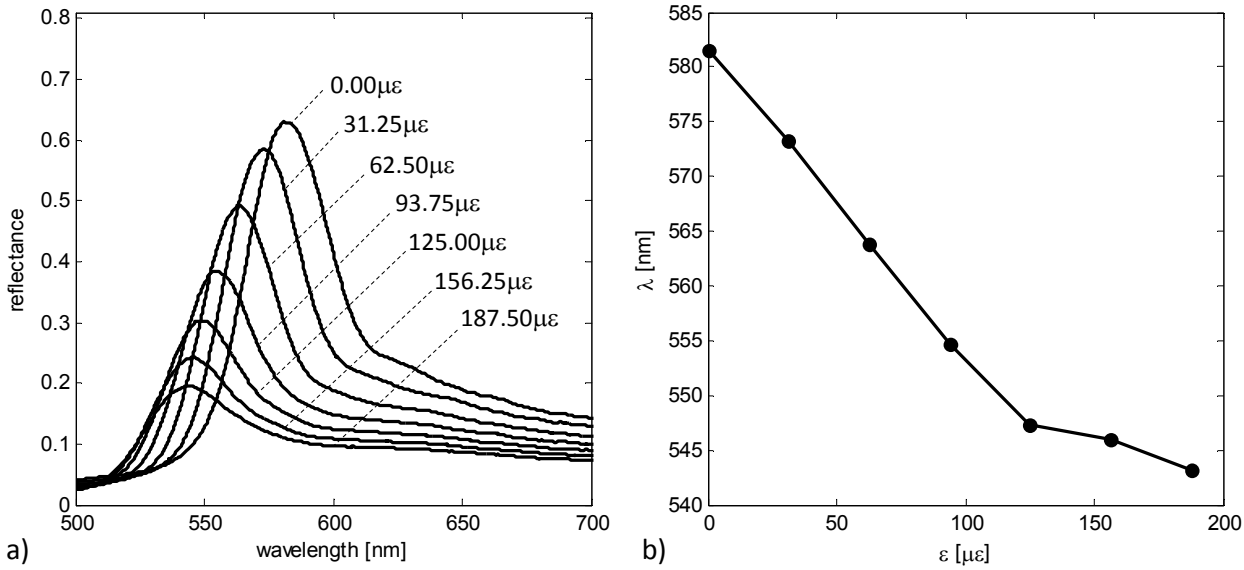

Figure 3. Reflectance spectra (a) of the colloidal PhC recorded during the elongation test and (b) experimental relationship between bandgap wavelength and strain.

If the maximum reflectance peak can be resolved with an accuracy of 0.1 nm, this corresponds to instrumental resolution of about 350 με. Such a resolution is acceptable for applications where the strain to be measured is a few percent. The latter circumstance though would invalidate the assumption of geometric linearity, namely infinitesimal strains, and also the material response would, at the very least, be nonlinearly elastic. Nonetheless such accuracy is actually not sufficient for civil and mechanical engineering applications, where often times the materials involved in the monitoring are steel and concrete, and so where a strain resolution the order of 5 με is typically required.

Equation (9) suggests that the resolution is easily improved by increasing the crystal interplanar spacing, for example by changing the size of the beads and/or by multiplying the swelling/infiltration cycles. However, this will result in a crystal which does not work in the visible range. Such a devise has then to be interrogated exclusively with instrumentation, thereby losing the feature that makes it appealing for monitoring applications.

4. FINITE DIFFERENCE TIME DOMAIN SIMULATIONS AND COMPARISON WITH THE EXPERIMENTAL RESULTS

In this section we provide a computational approach not only for validating our experimental results, but also for better understanding the behavior of this highly complex physical system, and pave the way to the design of innovative photonic sensors.

We employed one of the most popular technique for the solution of electromagnetic problems: the Finite Difference Time Domain (FDTD). It has been successfully applied to an extremely wide variety of problems, such as scattering from metal objects and dielectrics, antennas, microstrip circuits, and electromagnetic absorption in the human body exposed to radiation. The main reason of the success of the FDTD method resides in the fact that the method itself is extremely simple, even for programming a three-dimensional code, which is our case.

Having a 3D code is a key aspect for governing the multiphysics of our experiments, meaning the combination of the mechanics and the light interaction with matter.

The FDTD method works when the field equations of the Initial Boundary Value problem are written in their strong form. Indeed, to solve an electromagnetic problem, the idea is to simply discretize, both in time and space, the Maxwell's equations with central difference approximations.
Our group has already validated this numerical method in several other papers [15,16,17], writing our own code in order to better represent the physics of the problem involved.
In this paper, the modeled phenomenon is the progressive displacement of the PS spheres inside the PDMS matrix that represents, approximately, what happens to the device during our experiments. At each step, that stands for the position reached by the spheres during the deformation of the sample, the exciting signal is a linearly polarized plane wave pulse, injected on the FDTD grid by means of
the so called total-field/scattered-field (TF/SF) method that represents the monochromatic light beam.
The parameters for the model are taken the same as the ones described in section 3, but with the simplifying assumption of nonabsorbitive materials and no substrate under the crystal. The latter has a finite dimension in the z direction, meaning 12 planes, and it is infinite in the x and y directions.

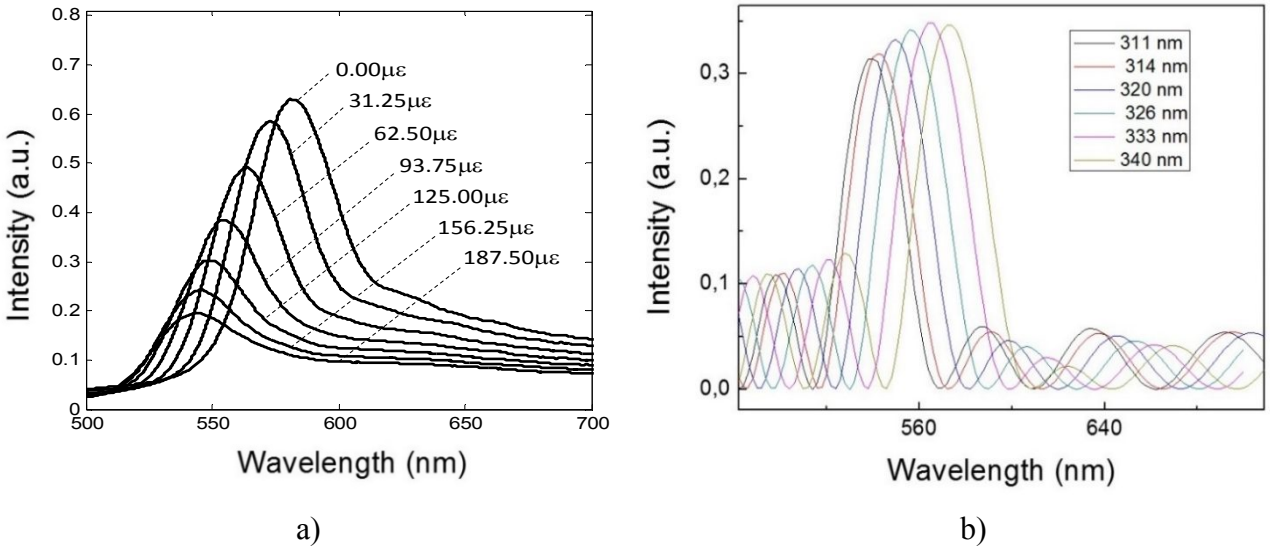

Figure 4. Reflectance spectra (a) of the colloidal PhC recorded during the elongation test of and (b) of the numerical simulations

As shown in Fig. 4, a) change in the reflectance is observed at every programmed step in which we vary the distance between the spheres, that means varying the lattice constant of the crystal structure (the values of the distance between the spheres is listed at the side of the graph a). A change in this latter parameter means a change in the geometry of the nanostructured device, which directly impact on the filling factor that in turn, as shown in formula (2), implies a change in the effective refractive index.
The effective refractive index plays a key role in the process of understanding the behavior of this kind of structure and it is the cause of several characteristic on both the experimental and numerical spectra.
Comparing the numerical results with the experimental ones, we see an agreement between the behavior of the simulated structure and the real sample. In fact, during the deformation of the sample, starting from a referential initial configuration in which the crystal is swelled, so the distance between the spheres in the z direction is maximum, in both cases there is a shift in the reflected wavelength from the higher to the lower ones. This effect is in agreement with the statement expressed in formula (7). In the numerical model the swelled configuration corresponds to the maximum value of the lattice constant, meaning approximately 340 nm. This shift shows also a decrease in the intensity, nonetheless the position peak is almost identical.
The decrease in the reflection intensity is proportional to the ratio between the difference of the refractive index of the materials (which is assumed to be constant in the model) and the effective refractive index as shown in the following formula [18].

$$I \propto \frac{\Delta n}{neff} \tag{11}$$

This demonstrates that the effective refractive index is changing due to the change in the volume fraction of the system, as it was highlighted above. Such a volume fraction for the FCC lattice can be evaluated as follows [19]:

$$f = \frac{2\pi}{3}\frac{d^3}{a^3} \tag{12}$$

where d is the diameter of the spheres and a is the lattice parameter ($a=d_{111}\sqrt{3}$).

A possible explanation for the fact that in the experiments the intensity decreases faster is that in the calculated numerical reflectance the absorbed power has been neglected because of the assumption of nonabsorbitive materials, in other words neglecting the imaginary component of the refractive index.

The asymmetry in the shape of the reflection spectra in the experiments is due to the cracks that are present into the sample [20]. The effects of this kind of defects is unavoidable while measuring, since the illuminated area is much larger (the unit are millimeters squared) than the domain without them (of the order of micrometers). Those cracks, which arises during the drying process of the PhC films, are not entirely avoidable and some other groups are working on this fabrication problem [21,22,23].

In terms of modeling the presence of such diffuse population of nano-cracks would entail the use of an advanced approach, which for now is beyond the scope of this research, as a much deeper characterization of the materials forming our composite would be required.

The shape of the experimental spectra changes also with the applied strain showing a broadening of it. This behavior is probably due to the coexistence of two phenomena that happen during the deformation of the sample: the opening of the cracks described above and an inhomogeneous differential displacement of the different planes of the crystal. This latter aspect could lead to an analogy with the reflectance spectra of a heterostructure [24,25,26], where there is the convolution of the contributions that every different inner structure gives. On the contrary, in the numerical results the broadening of the spectra is not present this could be explained with the assumption of a homothetic expansion of the spheres at each step, not taking into account the possibly arising inhomogeinity of the strain field in the matrix across neighboring spheres, boundary effects of the substrate into the crystals that could lead to a non-homogeneous displacements of the spheres in all directions and, obviously, the assumption of a perfect structure without any defects.

The issues just summarized suggest that more detailed modeling in terms of enriching the kinematics and the associated constitutive behavior would be required for future investigations, thereby leading to a much more complex code.

On a completely different notice, from the practical point of view the key aspect for SHM is the sensitivity of a strain sensor. As we highlighted in section 3, the sensitivity of our device was around 3.5 με /pm and it results in good agreement with the numerical one, which is around 3.85 με /pm. We can state with confidence that, not only from this point of view, the two systems are almost the same and the numerical model approximates at the best the experiment.

5. CONCLUSIONS

The presented results obtained by an approximate linear elastic model, with the further approximation of the homothetic expansion of the spheres, with no inhomogeinities on the strain field, is already in agreement with what we see experimentally and with the analytical model presented in section 2. The device has then a preliminary validation for the envisioned applications. A complete validation of the unit will require a lot more work to set up a robust understanding of the performances of the produced sensor, meaning significantly refining the modeling strategy. Overall, the examined 3D Photonic Crystal exhibits a lot of potential for the envisaged applications in Civil and Mechanical Engineering.

ACKNOWLEDGEMENTS

Large-scale simulations have been conducted on IBM BlueGene/Q supercomputer of the Southern Ontario Smart Computing Innovation Platform (SOSCIP).

REFERENCES

[1] R.M. Measures, *Structural monitoring with fiber optic technology*. Academic Press (2001).

[2] B. Glisic, D. Inaudi, *Fiber optic method for structural health monitoring*. Wiley (2007).

[3] M. Pozzi, D. Zonta, H. Wu, D. Inaudi, Development and laboratory validation of in-line multiplexed low-coherence interferometric sensors. *Optical Fiber Technology*, **14**, 281–293, 2008.

[4] D. Zonta, B. Glisic, S. Adriaenssens, Value of information: impact of monitoring on decision-making. *Structural Control and Health Monitoring,* **21**, 1043–1056, 2014.

[5] C. Cappello, D. Zonta, M. Pozzi, R. Zandonini, Impact of prior perception on bridge health diagnosis. *Journal of Civil Structural Health Monitoring*, **5**, 509–525, 2015.

[6] C. Cappello, D. Zonta, B. Glisic, Expected utility theory for monitoring-based decision making. *Proceedings of the IEEE*. In press, 2016.

[7] C. A. Sciarella, Overview of optical techniques that measure displacements: Murray lecture, Exp. Mech. 43(1), 2003.

[8] A. Chiappini, C. Armellini, A. Chiasera, M. Ferrari, Y. Jestin, M. Mattarelli, M. Montagna, E. Moser, G. Nunzi Conti, S. Pelli, G.C. Righini, M.C. Gonçalves, R.M. Almeida, Design of photonic structures by sol–gel-derived silica nanospheres, *J. of Non-Cryst. Solids*, **353**, 674-678, 2007.

[9] H. Fudouzi, T. Sawada, Photonic rubber sheets with tunable color by elastic deformation. *Langmuir*, **22**, 1365-1368, 2006.

[10] H. Fudouzi, Soft opal films with tunable structural color and their applications. Proc. SPIE **6005**, 22-30, 2005.

[11] D. Zonta, A. Chiappini, A. Chiasera, M. Ferrari, M. Pozzi, L. Battisti, M. Benedetti, Photonic crystals for monitoring fatigue phenomena in steel structures. Proc. SPIE 7292, 729215/1-10, 2008.

[12] Z.M. Wang, A. Neogi, *Nanoscale Photonics and Optoelectronics*. Springer, 65-69, 2010.

[13] R.M. Almeida, S. Portal, Photonic band gap structure by sol-gel processing. *Curr. Opin. Solid St. M.,* **7**, 151-157, 2003.

[14] A. Chiappini, A. Piotrowska, M. Marciniak, M. Ferrari M. and D. Zonta, Design and fabrication of mechanochromic photonic crystals as strain sensor. Proc. SPIE. **9435**, 94350J-1/13, 2015.

[15] A. Vaccari, A. Calà Lesina, L. Cristoforetti, A. Chiappini, F. Prudenzano, A. Bozzoli, and M. Ferrari, A parallel computational FDTD approach to the analysis of the light scattering from an opal photonic crystal, Proc. SPIE **8781**, 87810P-1/6, 2013.

[16] A. Vaccari, L. Cristoforetti, A. Calà Lesina, L. Ramunno, A. Chiappini, F. Prudenzano, A. Bozzoli, L. Calliari, Parallel finite-difference time-domain modeling of an opal photonic crystal, Optical Engineering 53, 071809-1/6, 2014.

[17] A. Vaccari, A. Calà Lesina, L. Cristoforetti, A. Chiappini, L. Crema, L. Calliari, L. Ramunno, P. Berini, and M. Ferrari, Light-opals interaction modeling by direct numerical solution of Maxwell's equations, Optics Express **22,** 27739-27749, 2014.

[18] T. Ding, S. K. Smoukov, and J. J. Baumberg, Stamping colloidal photonic crystals: a facile way towards complex pixel colour patterns for sensing and displays, Nanoscale, DOI: 10.1039/c4nr05934d, 2014.

[19] R. D. Pradhan, I. I. Tarhan, and G. H. Watson, Impurity modes in the optical stop bands of doped colloidal crystals, Phys. Rev. B, Vol 54, No 19, 1996.

[20] Y. A. Vlasov, V. N. Astratov, A. V. Baryshev, A. A. Kaplyanskii, O. Z. Karimov, and M. F. Limonov, Manifestation of intrinsic defects in optical properties of self-organized opal photonic crystals, Phys. Rev. E, vol 61, no 5, 2000.

[21] B. Hatton, L. Mishchenko, S. Davis, K. H. Sandhage and J. Aizenberg, Proc. Natl. Acad. Sci. U. S. A., 107, 2010.

[22] J. Zhou, J. Wang, Y. Huang, G. Liu, L. Wang, S. Chen, X. Li, D. Wang, Y. Song and L. Jiang, NPG Asia Mater., 4, 2012.

[23] Y. Huang, J. Zhou, B. Su, L. Shi, J. Wang, S. Chen, L. Wang, J. Zi, Y. Song and L. Jiang, J. Am. Chem. Soc., 134, 2012.

[24] H. S. Lee, R. Kubrin, R. Zierold, A. Y. Petrov, K. Nielsch, G. A. Schneider, and M. Eich, Photonic properties of titania inverse opal heterostructures, Optical Material Express, Vol 3, No 8, 2013.

[25] A. Chiappini, C. Armellini, N. Bazzanella, G. C. Righini, M. Ferrari, Opal-based photonic crystals heterostructures, Optics and Photonic Journal **2**, 206-210, 2012.

[26] D. K. Hwang, H. Noh, H. Cao, and R. P. H. Chang, Photonic bandgap engineering with inverse opal multi-stacks of different refractive index contrast, Appl. Phys. Lett., **95**, 2009.